

Study of double charmonium production in e^+e^- annihilation at $\sqrt{s} \approx 10.6$ GeV

K. Abe,⁸ K. Abe,³⁹ H. Aihara,⁴¹ Y. Asano,⁴⁴ V. Aulchenko,¹ T. Aushev,¹² S. Bahinipati,⁴ A. M. Bakich,³⁶ Y. Ban,³² I. Bedny,¹ U. Bitenc,¹³ I. Bizjak,¹³ S. Blyth,²⁵ A. Bondar,¹ A. Bozek,²⁶ M. Bračko,^{19,13} J. Brodzicka,²⁶ T. E. Browder,⁷ Y. Chao,²⁵ B. G. Cheon,³ R. Chistov,¹² S.-K. Choi,⁶ Y. Choi,³⁵ A. Chuvikov,³³ S. Cole,³⁶ M. Danilov,¹² M. Dash,⁴⁵ L. Y. Dong,¹⁰ S. Eidelman,¹ V. Eiges,¹² F. Fang,⁷ S. Fratina,¹³ N. Gabyshev,¹ T. Gershon,⁸ G. Gokhroo,³⁷ B. Golob,^{18,13} R. Guo,²³ J. Haba,⁸ N. C. Hastings,⁸ K. Hayasaka,²¹ H. Hayashii,²² M. Hazumi,⁸ T. Higuchi,⁸ L. Hinz,¹⁷ T. Hokuue,²¹ Y. Hoshi,³⁹ W.-S. Hou,²⁵ Y. B. Hsiung,^{25,*} T. Iijima,²¹ A. Imoto,²² K. Inami,²¹ A. Ishikawa,⁸ R. Itoh,⁸ H. Iwasaki,⁸ M. Iwasaki,⁴¹ Y. Iwasaki,⁸ J. H. Kang,⁴⁶ J. S. Kang,¹⁵ N. Katayama,⁸ H. Kawai,² T. Kawasaki,²⁸ H. R. Khan,⁴² H. J. Kim,¹⁶ P. Koppenburg,⁸ P. Križan,^{18,13} P. Krokovny,¹ S. Kumar,³¹ Y.-J. Kwon,⁴⁶ J. S. Lange,⁵ G. Leder,¹¹ T. Lesiak,²⁶ J. Li,³⁴ S.-W. Lin,²⁵ J. MacNaughton,¹¹ G. Majumder,³⁷ F. Mandl,¹¹ T. Matsumoto,⁴³ A. Matyja,²⁶ W. Mitaroff,¹¹ H. Miyake,³⁰ H. Miyata,²⁸ R. Mizuk,¹² T. Mori,⁴² T. Nagamine,⁴⁰ Y. Nagasaka,⁹ E. Nakano,²⁹ M. Nakao,⁸ Z. Natkaniec,²⁶ S. Nishida,⁸ T. Nozaki,⁸ S. Ogawa,³⁸ T. Ohshima,²¹ T. Okabe,²¹ S. Okuno,¹⁴ S. L. Olsen,⁷ W. Ostrowicz,²⁶ H. Ozaki,⁸ P. Pakhlov,¹² H. Palka,²⁶ C. W. Park,¹⁵ H. Park,¹⁶ N. Parslow,³⁶ L. S. Peak,³⁶ L. E. Piilonen,⁴⁵ H. Sagawa,⁸ Y. Sakai,⁸ N. Sato,²¹ O. Schneider,¹⁷ J. Schümann,²⁵ S. Semenov,¹² K. Senyo,²¹ R. Seuster,⁷ M. E. Sevir,²⁰ H. Shibuya,³⁸ V. Sidorov,¹ A. Somov,⁴ N. Soni,³¹ R. Stamen,⁸ S. Stanič,^{44,†} M. Starič,¹³ K. Sumisawa,³⁰ T. Sumiyoshi,⁴³ O. Tajima,⁴⁰ F. Takasaki,⁸ K. Tamai,⁸ N. Tamura,²⁸ M. Tanaka,⁸ G. N. Taylor,²⁰ Y. Teramoto,²⁹ K. Trabelsi,⁷ T. Tsuboyama,⁸ T. Tsukamoto,⁸ S. Uehara,⁸ T. Uglov,¹² K. Ueno,²⁵ Y. Unno,² S. Uno,⁸ G. Varner,⁷ K. E. Varvell,³⁶ C. C. Wang,²⁵ C. H. Wang,²⁴ M. Watanabe,²⁸ B. D. Yabsley,⁴⁵ Y. Yamada,⁸ A. Yamaguchi,⁴⁰ Y. Yamashita,²⁷ M. Yamauchi,⁸ S. L. Zang,¹⁰ C. C. Zhang,¹⁰ J. Zhang,⁸ Z. P. Zhang,³⁴ and D. Žontar^{18,13}

(Belle Collaboration)

¹*Budker Institute of Nuclear Physics, Novosibirsk*

²*Chiba University, Chiba*

³*Chonnam National University, Kwangju*

⁴*University of Cincinnati, Cincinnati, Ohio 45221*

⁵*University of Frankfurt, Frankfurt*

⁶*Gyeongsang National University, Chinju*

⁷*University of Hawaii, Honolulu, Hawaii 96822*

⁸*High Energy Accelerator Research Organization (KEK), Tsukuba*

⁹*Hiroshima Institute of Technology, Hiroshima*

¹⁰*Institute of High Energy Physics, Chinese Academy of Sciences, Beijing*

¹¹*Institute of High Energy Physics, Vienna*

¹²*Institute for Theoretical and Experimental Physics, Moscow*

¹³*J. Stefan Institute, Ljubljana*

¹⁴*Kanagawa University, Yokohama*

¹⁵*Korea University, Seoul*

¹⁶*Kyungpook National University, Taegu*

¹⁷*Swiss Federal Institute of Technology of Lausanne, EPFL, Lausanne*

¹⁸*University of Ljubljana, Ljubljana*

¹⁹*University of Maribor, Maribor*

²⁰*University of Melbourne, Victoria*

²¹*Nagoya University, Nagoya*

²²*Nara Women's University, Nara*

²³*National Kaohsiung Normal University, Kaohsiung*

²⁴*National United University, Miao Li*

²⁵*Department of Physics, National Taiwan University, Taipei*

²⁶*H. Niewodniczanski Institute of Nuclear Physics, Krakow*

²⁷*Nihon Dental College, Niigata*

²⁸*Niigata University, Niigata*

²⁹*Osaka City University, Osaka*

³⁰*Osaka University, Osaka*

³¹*Panjab University, Chandigarh*

³²*Peking University, Beijing*

³³*Princeton University, Princeton, New Jersey 08545*

³⁴*University of Science and Technology of China, Hefei*

³⁵*Sungkyunkwan University, Suwon*³⁶*University of Sydney, Sydney NSW*³⁷*Tata Institute of Fundamental Research, Bombay*³⁸*Toho University, Funabashi*³⁹*Tohoku Gakuin University, Tagajo*⁴⁰*Tohoku University, Sendai*⁴¹*Department of Physics, University of Tokyo, Tokyo*⁴²*Tokyo Institute of Technology, Tokyo*⁴³*Tokyo Metropolitan University, Tokyo*⁴⁴*University of Tsukuba, Tsukuba*⁴⁵*Virginia Polytechnic Institute and State University, Blacksburg, Virginia 24061*⁴⁶*Yonsei University, Seoul*

(Received 5 July 2004; published 25 October 2004)

We present a new analysis of double charmonium production in e^+e^- annihilation. The observation of the processes $e^+e^- \rightarrow J/\psi\eta_c$, $J/\psi\chi_{c0}$, and $J/\psi\eta_c(2S)$ is confirmed using a data set more than 3 times larger than that of Belle's previous report, and no evidence for the process $e^+e^- \rightarrow J/\psi J/\psi$ is found. We perform an angular analysis for $J/\psi\eta_c$ production and set an upper limit on the production of $J/\psi J/\psi$. Processes of the type $e^+e^- \rightarrow \psi(2S)(c\bar{c})_{\text{res}}$ have been observed for the first time; their rates are found to be comparable to those of $e^+e^- \rightarrow J/\psi(c\bar{c})_{\text{res}}$ processes.

DOI: 10.1103/PhysRevD.70.071102

PACS numbers: 13.66.Bc, 12.38.Bx, 14.40.Gx

The large rate for processes of the type $e^+e^- \rightarrow J/\psi\eta_c$ and $J/\psi(c\bar{c})_{\text{non-res}}$ reported by Belle [1] remains unexplained. Following the publication of this result, the cross section for $e^+e^- \rightarrow J/\psi\eta_c$ via e^+e^- annihilation into a single virtual photon was calculated using nonrelativistic QCD (NRQCD) to be ~ 2 fb [2], which is at least an order of magnitude smaller than the measured value. Several hypotheses have been suggested in order to resolve this discrepancy. In particular, the authors of Ref. [3] have proposed that processes proceeding via two virtual photons may be important. Other authors [4] suggest that since the dominant mechanism for charmonium production in e^+e^- annihilation is expected to be the color-singlet process $e^+e^- \rightarrow c\bar{c}g\bar{g}$, the final states observed by Belle contain a charmonium state and a $M \sim 3$ GeV/ c^2 glueball. Such glueball states are predicted by lattice QCD and can have masses around 3 GeV/ c^2 . Possible glueball contributions to the χ_{c0} signal are also discussed in Ref. [5].

The previous Belle analysis was performed with a data sample of 45 fb $^{-1}$. The process $e^+e^- \rightarrow J/\psi\eta_c$ was inferred from the η_c peak in the mass spectrum of the system recoiling against the reconstructed J/ψ in inclusive $e^+e^- \rightarrow J/\psi X$ events. In this paper we report an extended analysis of the $e^+e^- \rightarrow J/\psi(c\bar{c})_{\text{res}}$ process to check the above hypotheses and provide extra information that might be useful to resolve the puzzle. This study is performed using a data sample of 140 fb $^{-1}$ collected at the $Y(4S)$ resonance and 15 fb $^{-1}$ at an energy 60 MeV below the $Y(4S)$. The data were collected with the Belle

detector [6] at the KEKB asymmetric energy e^+e^- storage rings [7].

The analysis procedure is described in detail in Ref. [1]. For J/ψ reconstruction we combine oppositely charged tracks that are both positively identified either as muons or electrons. For $J/\psi \rightarrow e^+e^-$, the invariant mass calculation includes the four-momentum of photons detected within 50 mrad of the e^\pm directions, as a partial correction for final state radiation and bremsstrahlung energy loss. The $J/\psi \rightarrow \ell^+\ell^-$ signal region is defined by a mass window $|M_{\ell^+\ell^-} - M_{J/\psi}| < 30$ MeV/ c^2 ($\approx 2.5\sigma_M$). QED processes are significantly suppressed by the requirement that the total charged multiplicity (N_{ch}) in the event be $N_{\text{ch}} > 4$. The contribution from J/ψ mesons in $B\bar{B}$ events is removed by requiring the center-of-mass (CM) momentum $p_{J/\psi}^*$ to be greater than 2.0 GeV/ c . A mass-constrained fit is then performed to improve the $p_{J/\psi}^*$ resolution and the recoil mass $M_{\text{recoil}} = \sqrt{(E_{\text{CM}} - E_{J/\psi}^*)^2 - p_{J/\psi}^{*2}}$ is calculated, where $E_{J/\psi}^*$ is the J/ψ CM energy after the mass constraint. $\psi(2S)$ is reconstructed via its decay to $J/\psi\pi^+\pi^-$ and the $\psi(2S)$ signal window is defined as $|M_{J/\psi\pi^+\pi^-} - M\{\psi(2S)\}| < 10$ MeV/ c^2 ($\approx 3\sigma_M$).

The $M_{\text{recoil}}(J/\psi)$ spectrum for the data is presented in Fig. 1: clear peaks around the nominal η_c and χ_{c0} masses are evident; another significant peak around ~ 3.63 GeV/ c^2 is identified as the $\eta_c(2S)$. The authors of Ref. [3] estimated that the two-photon-mediated process $e^+e^- \rightarrow J/\psi J/\psi$ has a significant cross section and suggested that the observed $e^+e^- \rightarrow J/\psi\eta_c$ signal in [1] might also include double J/ψ events, thereby producing an inflated cross section measurement. Since e^+e^- annihilation to $J/\psi J/\psi$ via a single virtual photon is forbid-

*On leave from Fermi National Accelerator Laboratory, Batavia, IL 60510, USA

†On leave from Nova Gorica Polytechnic, Nova Gorica

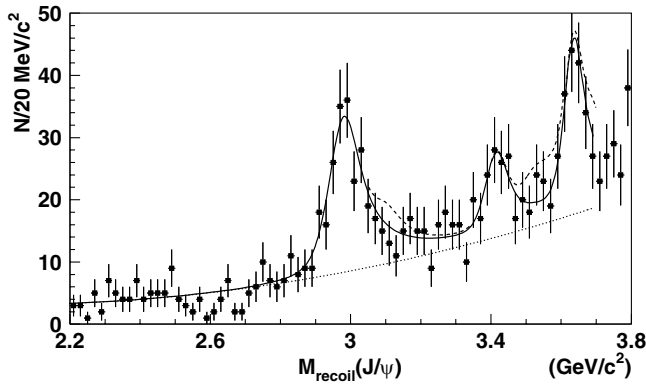


FIG. 1. The mass of the system recoiling against the reconstructed J/ψ in inclusive $e^+e^- \rightarrow J/\psi X$ events. The curves are described in the text.

den by charge conjugation symmetry, it was ignored in our previous analysis. To allow for a possible contribution from the exchange of two virtual photons, we fit the spectrum in Fig. 1 including all of the known narrow charmonium states. In this fit, the mass positions for the η_c , χ_{c0} , and $\eta_c(2S)$ are free parameters; those for the J/ψ , χ_{c1} , χ_{c2} , and $\psi(2S)$ are fixed at their nominal values. The expected line-shapes for these peaks are determined from a Monte Carlo (MC) simulation as described in our previous paper [1], the background is parametrized by a second order polynomial function, and only the region below the open charm threshold ($M_{\text{recoil}} < 3.7 \text{ GeV}/c^2$) is included in the fit. The fit results are listed in Table I; the $\chi^2/n.d.f.$ of the fit is equal to 0.88. The yields for η_c , χ_{c0} , and $\eta_c(2S)$ have statistical significances between 3.8 and 10.7. The significance of each signal is defined as $\sqrt{-2 \ln(\mathcal{L}_0/\mathcal{L}_{\text{max}})}$, where \mathcal{L}_0 and \mathcal{L}_{max} denote the likelihoods with the corresponding signal yield fixed at zero and at the best-fit value, respectively. The fit returns negative yields for the J/ψ and $\psi(2S)$; the χ_{c1} and χ_{c2} yields are found to be consistent with zero. A fit with all these contributions fixed at zero is shown as a solid line in Fig. 1; the difference in the η_c , χ_{c0} , and $\eta_c(2S)$ yields

TABLE I. Summary of the signal yields (N), charmonium masses (M), significances, and cross sections ($\sigma_{\text{Born}} \times \mathcal{B}_{>2}[(c\bar{c})_{\text{res}}]$) for $e^+e^- \rightarrow J/\psi(c\bar{c})_{\text{res}}$; $\mathcal{B}_{>2}$ denotes the branching fraction for final states with more than two charged tracks.

$(c\bar{c})_{\text{res}}$	N	$M [\text{GeV}/c^2]$	Signif.	$\sigma_{\text{Born}} \times \mathcal{B}_{>2} [\text{fb}]$
η_c	235 ± 26	2.972 ± 0.007	10.7	$25.6 \pm 2.8 \pm 3.4$
J/ψ	-14 ± 20	fixed	...	<9.1 at 90% CL
χ_{c0}	89 ± 24	3.407 ± 0.011	3.8	$6.4 \pm 1.7 \pm 1.0$
$\chi_{c1} + \chi_{c2}$	10 ± 27	fixed	...	<5.3 at 90% CL
$\eta_c(2S)$	164 ± 30	3.630 ± 0.008	6.0	$16.5 \pm 3.0 \pm 2.4$
$\psi(2S)$	-26 ± 29	fixed	...	<13.3 at 90% CL

compared to the default fit is small, and is included in the systematic errors. The dashed line in the figure corresponds to the case where the contributions of the J/ψ , χ_{c1} , χ_{c2} , and $\psi(2S)$ are set at their 90% confidence level (CL) upper limit values. The dotted line is the background function.

Given the arguments in Ref. [3], it is important to check for any momentum scale bias that may shift the recoil mass values and confuse the interpretation of peaks in the M_{recoil} spectrum. We use $e^+e^- \rightarrow \psi(2S)\gamma$, $\psi(2S) \rightarrow J/\psi\pi^+\pi^-$ events to calibrate and verify the recoil mass scale. Events with a reconstructed $\psi(2S)$ and with no other charged tracks form a pure $e^+e^- \rightarrow \psi(2S)\gamma$ sample with less than 1% background as estimated using the $\psi(2S)$ sideband region. We use the $\psi(2S)$ momentum to calculate the square of the mass of the recoiling system; the resulting spectrum is shown in Fig. 2. The scaled $\psi(2S)$ sideband is also shown. We perform a fit to the $M_{\text{recoil}}^2[\psi(2S)]$ spectrum, using Monte Carlo simulation to determine the expected signal shape; second order QED corrections, which produce a higher M_{recoil}^2 tail, are taken into account. The peak position is left free in the fit and the non- $\psi(2S)$ background is ignored. The fit finds the shift in the data with respect to the MC function to be consistent with zero, $\Delta M_{\text{recoil}}^2 = 0.010 \pm 0.009 \text{ GeV}^2/c^4$. In MC events, we introduce a bias into the J/ψ momentum scale that creates a shift equal to the corresponding 90% CL upper limit, $\Delta M_{\text{recoil}}^2[\psi(2S)] = 0.025 \text{ GeV}^2/c^4$; we find that this bias causes a J/ψ recoil mass shift of $\sim 3 \text{ MeV}/c^2$ for $M_{\text{recoil}}(J/\psi)$ values near $3 \text{ GeV}/c^2$. From this study we conclude that the J/ψ recoil mass is shifted by not more than $3 \text{ MeV}/c^2$ in the region of interest.

As an additional cross-check we fully reconstruct double charmonium events. The η_c is reconstructed as $K_S^0 K^\pm \pi^\mp$ ($K_S^0 \rightarrow \pi^+ \pi^-$) or $2(K^+ K^-)$ combinations

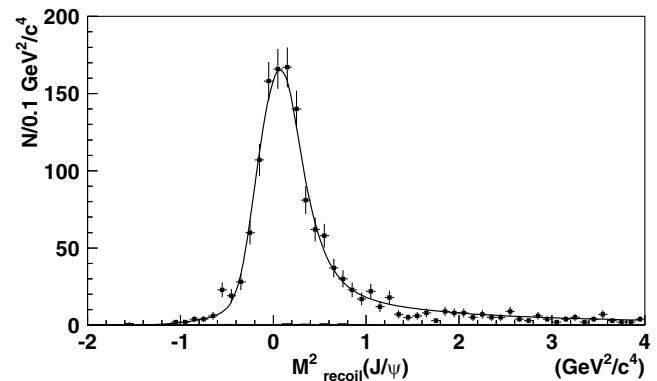


FIG. 2. The square of the mass of the system recoiling against the reconstructed $\psi(2S) \rightarrow J/\psi\pi^+\pi^-$, in events with charged multiplicity equal to four. Points with error bars show the data; the solid line shows the result of the fit described in the text. The hatched histogram (scarcely visible) shows the spectrum in the scaled $\psi(2S)$ sidebands.

K. ABE *et al.*

within a window of ± 50 MeV/ c^2 around the nominal η_c mass. In events with $N_{\text{ch}} = 6$ we find three events with $J/\psi\eta_c$ combinations in a ± 100 MeV window around the CM energy ($\approx 3\sigma$). No events are seen in the η_c sideband region ($100 < M[K_S K \pi/2(KK)] - M_{\eta_c} < 350$ MeV); a fit to the mass distribution gives an η_c signal significance of 4.1σ . Based on the η_c yield in the $M_{\text{recoil}}(J/\psi)$ distribution, we expect 2.6 ± 0.8 fully reconstructed events, consistent with the observed signal. Thus we conclude that the peak in $M_{\text{recoil}}(J/\psi)$ is dominated by η_c production. We also search for fully reconstructed double J/ψ candidates in events with $N_{\text{ch}} = 4$. No $J/\psi J/\psi$ candidates are found in a window of ± 100 MeV around the CM energy.

Based on the calibration of the $M_{\text{recoil}}(J/\psi)$ scale, the result of the fit to the $M_{\text{recoil}}(J/\psi)$ distribution and the full reconstruction cross-check, we confirm our published observation of the process $e^+e^- \rightarrow J/\psi\eta_c$ and rule out the suggestion of Ref. [3] that a significant fraction of the inferred $J/\psi\eta_c$ signal might be due to $J/\psi J/\psi$ events.

The reconstruction efficiencies for the $J/\psi\eta_c$, $J/\psi\chi_{c0}$, and $J/\psi\eta_c(2S)$ final states strongly depend on θ_{prod} , the production angle of the J/ψ in the CM frame with respect to the beam axis, and the helicity angle θ_{hel} , defined as the angle between the decay ℓ^+ direction and the boost direction of the CM frame in the J/ψ rest frame. We therefore perform an angular analysis for these modes before computing cross sections. We fit the $M_{\text{recoil}}(J/\psi)$ distributions in bins of $|\cos(\theta_{\text{prod}})|$, and correct the yield for the bin-by-bin reconstruction efficiency determined from the MC [8]; the same procedure is followed for $|\cos(\theta_{\text{hel}})|$. The reconstruction efficiencies in bins of each variable are shown in Fig. 3. The efficiency corrected yields in the data are plotted in Fig. 4, together with fits to functions $A(1 + \alpha\cos^2\theta)$ (solid lines). We also perform simultaneous fits to the production and helicity angle distributions for each of the $(c\bar{c})_{\text{res}}$ states, assuming $J/\psi(c\bar{c})_{\text{res}}$ production via a single virtual photon and angular momentum conservation, thus setting $\alpha_{\text{prod}} \equiv \alpha_{\text{hel}}$. The values of the parameter α from the separate

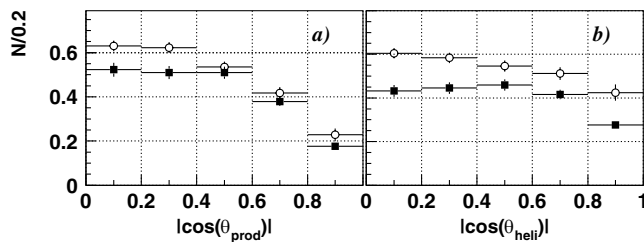


FIG. 3. Dependence of the reconstruction efficiencies on cosines of the production (a) and J/ψ helicity angles (b) for $e^+e^- \rightarrow J/\psi\eta_c[\eta_c(2S)]$ (solid squares) and $e^+e^- \rightarrow J/\psi\chi_{c0}$ (open circles).

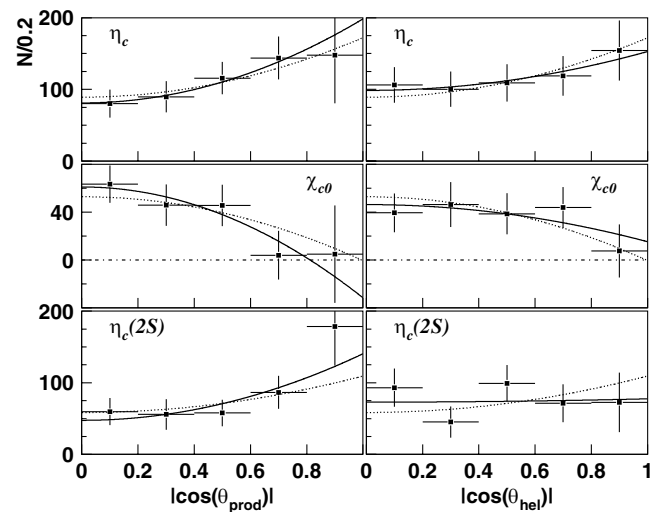


FIG. 4. Distributions of cosines of the production (left) and J/ψ helicity angles (right) for $e^+e^- \rightarrow J/\psi\eta_c$ (top row), $e^+e^- \rightarrow J/\psi\chi_{c0}$ (middle row), and $e^+e^- \rightarrow J/\psi\eta_c(2S)$ (bottom row). The solid lines are results of the individual fits; the dotted lines are the simultaneous fit results.

fits to $|\cos(\theta_{\text{hel}})|$ and $|\cos(\theta_{\text{prod}})|$, and from the simultaneous fits, are listed in Table II.

The angular distributions for the $J/\psi\eta_c$ and $J/\psi\eta_c(2S)$ peaks are consistent with the expectations for production of these final states via a single virtual photon, $\alpha_{\text{prod}} = \alpha_{\text{hel}} = +1$ [2]. There is no evidence for the sharp rise in cross section for large $|\cos(\theta_{\text{prod}})|$ expected for $J/\psi J/\psi$ production via two virtual photons [3]. The prediction for a spin-0 glueball contribution ($e^+e^- \rightarrow J/\psi\mathcal{G}_0$) to the $J/\psi\eta_c$ peak, $\alpha_{\text{prod}} = \alpha_{\text{hel}} \approx -0.87$ [4], is also disfavored.

The process $e^+e^- \rightarrow \gamma^* \rightarrow J/\psi\chi_{c0}$ can proceed via both S- and D-wave amplitudes, and predictions for the resulting angular distributions are therefore model dependent. Our results disfavor the NRQCD expectation $\alpha_{\text{prod}} = \alpha_{\text{hel}} \approx 0.25$ [2,5], and are more consistent with S-wave production, where $\alpha_{\text{prod}} = \alpha_{\text{hel}} = -1$.

To calculate the cross sections for the processes $e^+e^- \rightarrow J/\psi\eta_c, J/\psi\chi_{c0}, J/\psi\eta_c(2S)$ we fix the production and helicity angle distributions in the MC to $1 + \cos^2\theta$ for $J/\psi\eta_c[\eta_c(2S)]$, and to $1 - \cos^2\theta$ for $J/\psi\chi_{c0}$.

TABLE II. The α parameters obtained from fits to the production and helicity angle distributions for $e^+e^- \rightarrow J/\psi(c\bar{c})_{\text{res}}$.

$(c\bar{c})_{\text{res}}$	Separate fits		Simultaneous fits
	α_{prod}	α_{hel}	$\alpha_{\text{hel}} \equiv \alpha_{\text{prod}}$
η_c	$1.4^{+1.1}_{-0.8}$	$0.5^{+0.7}_{-0.5}$	$0.93^{+0.57}_{-0.47}$
χ_{c0}	-1.7 ± 0.5	$-0.7^{+0.7}_{-0.5}$	$-1.01^{+0.38}_{-0.33}$
$\eta_c(2S)$	$1.9^{+2.0}_{-1.2}$	$0.3^{+1.0}_{-0.7}$	$0.87^{+0.86}_{-0.63}$

The statistical errors in the α parameters for the angular distributions are translated into uncertainties in the efficiency determination and included in the systematic error. To set a conservative upper limit for $e^+e^- \rightarrow J/\psi J/\psi, J/\psi \chi_{c1(2)}, J/\psi \psi(2S)$, we use assumptions for the production and helicity angle distributions that correspond to the lowest detection efficiency. Note that for $J/\psi J/\psi$ and $J/\psi \psi(2S)$ the assumed angular distributions lead to lower efficiencies than those that follow from the predictions of Ref. [3].

To reduce the model dependence of our results due to the effect of initial state radiation (ISR), whose form-factor dependence on Q^2 of the virtual photon is unknown, we calculate cross sections in the Born approximation. We first calculate the fraction of events in the signal $M_{\text{recoil}}(J/\psi)$ distributions that are accompanied by an ISR photon of an energy smaller than a cutoff E_{cutoff} using MC. We then correct the cross sections calculated for that cutoff value using a factor that yields the Born cross section [9]. The final result ($\sigma_{\text{Born}} = 0.70 \cdot \sigma_{\text{full}}$) is then independent of the choice of the cutoff energy provided E_{cutoff} satisfies $M_e \ll E_{\text{cutoff}} \ll E_{\text{CM}}$. As in Ref. [1], because of selection criteria we present our result in terms of the product of the cross section and the branching fraction of the recoil charmonium state into more than two charged tracks: $\sigma \times \mathcal{B}_{>2}$, where $\mathcal{B}_{>2}[(c\bar{c})_{\text{res}}] \equiv \mathcal{B}[(c\bar{c})_{\text{res}} \rightarrow >2 \text{ charged}]$. The cross sections are given in Table I.

We perform a similar study with reconstructed $\psi(2S) \rightarrow J/\psi \pi^+ \pi^-$ decays to search for $e^+e^- \rightarrow \psi(2S)(c\bar{c})_{\text{res}}$ processes. The recoil mass spectrum for the data is presented in Fig. 5: peaks corresponding to the η_c, χ_{c0} , and $\eta_c(2S)$ can be seen. The fit to the $M_{\text{recoil}}[\psi(2S)]$ distribution is identical to the $M_{\text{recoil}}(J/\psi)$ fit, but due to the limited sample in this case, the masses of the established charmonium states are fixed to their nominal values; the $\eta_c(2S)$ mass is fixed to 3.630 GeV/ c^2 as found from the $M_{\text{recoil}}(J/\psi)$ fit. The signal yields are listed in

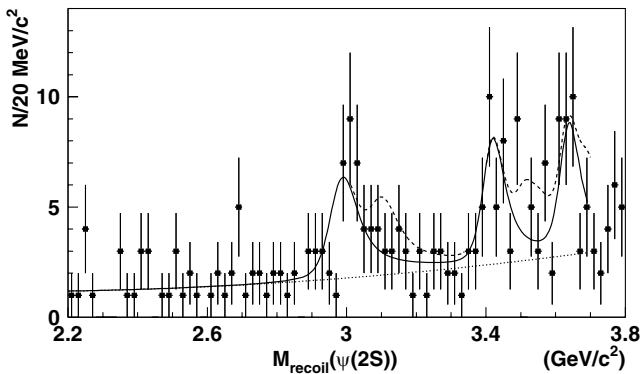


FIG. 5. The mass of the system recoiling against the reconstructed $\psi(2S)$ in inclusive $e^+e^- \rightarrow \psi(2S)X$ events. The curves are described in the text.

TABLE III. Summary of the signal yields (N), significances, and cross sections ($\sigma_{\text{Born}} \times \mathcal{B}_{>0}[(c\bar{c})_{\text{res}}]$) for $e^+e^- \rightarrow \psi(2S) \times (c\bar{c})_{\text{res}}$; $\mathcal{B}_{>0}$ denotes the branching fraction for final states containing charged tracks.

$(c\bar{c})_{\text{res}}$	N	Signif.	$\sigma_{\text{Born}} \times \mathcal{B}_{>0}$ [fb]
η_c	36.7 ± 10.4	4.2	$16.3 \pm 4.6 \pm 3.9$
J/ψ	6.9 ± 8.9	...	<16.9 at 90% CL
χ_{c0}	35.4 ± 10.7	3.5	$12.5 \pm 3.8 \pm 3.1$
$\chi_{c1} + \chi_{c2}$	6.6 ± 8.0	...	<8.6 at 90% CL
$\eta_c(2S)$	36.0 ± 11.4	3.4	$16.0 \pm 5.1 \pm 3.8$
$\psi(2S)$	-8.3 ± 8.5	...	<5.2 at 90% CL

Table III; the $\chi^2/n.d.f.$ of the fit is equal to 0.86. Significances for the individual η_c, χ_{c0} , and $\eta_c(2S)$ peaks are in the range $3 \sim 4\sigma$; the significance for $e^+e^- \rightarrow \psi(2S)(c\bar{c})_{\text{res}}$, where $(c\bar{c})_{\text{res}}$ is a sum over η_c, χ_{c0} , and $\eta_c(2S)$, is estimated to be 5.3σ . The significance is calculated as $\sqrt{-2 \ln(\mathcal{L}_0/\mathcal{L}_{\text{max}})}$, where \mathcal{L}_0 and \mathcal{L}_{max} denote the likelihoods of the fit with all signal yields fixed at zero and at the best-fit value, respectively. In Fig. 5 the result of a fit with only η_c, χ_{c0} , and $\eta_c(2S)$ contributions included is shown as a solid line; the dashed line shows the case where the $J/\psi, \chi_{c1}, \chi_{c2}$, and $\psi(2S)$ contributions are set at their 90% confidence level upper limit values. The dotted line is the background function.

To estimate the efficiency we assume the $\psi(2S)$ production and helicity angle distributions to be the same as those for the corresponding $J/\psi(c\bar{c})_{\text{res}}$ final states. Finally, the calculated products of the Born cross section and the branching fraction of the recoiling charmonium state into two or more charged tracks ($\sigma \times \mathcal{B}_{>0}$, where $\mathcal{B}_{>0}[(c\bar{c})_{\text{res}}] \equiv \mathcal{B}[(c\bar{c})_{\text{res}} \rightarrow >0 \text{ charged}]$) are presented in Table III.

The systematic error is dominated by the fitting systematics of the signal yields: 10% for $J/\psi(c\bar{c})_{\text{res}}$ and 14% for $\psi(2S)(c\bar{c})_{\text{res}}$. To estimate this contribution we vary the parametrizations of the signal (intrinsic widths of charmonium states, form-factor dependence on Q^2) and background in the fit to the M_{recoil} spectra. Another large contribution is due to the reconstruction efficiency dependence on the angular distributions [7% for $J/\psi(c\bar{c})_{\text{res}}$ and 15% for $\psi(2S)(c\bar{c})_{\text{res}}$]. In the MC, the angular parameters α are varied within the statistical errors of our angular analysis for $e^+e^- \rightarrow J/\psi(c\bar{c})_{\text{res}}$ and in the full range $[-1 \leq \alpha_{\text{prod}}(\alpha_{\text{hel}}) \leq 1]$ for $e^+e^- \rightarrow \psi(2S)(c\bar{c})_{\text{res}}$ to estimate the uncertainty in efficiencies. Other contributions for $e^+e^- \rightarrow J/\psi(c\bar{c})_{\text{res}}$ [$\psi(2S)(c\bar{c})_{\text{res}}$] come from the multiplicity cut [3%(2%)], track reconstruction efficiency [3%(5%)] and lepton identification [3%(3%)].

In summary, using a larger data set we confirm our published observation of $e^+e^- \rightarrow J/\psi \eta_c, J/\psi \chi_{c0}$

and $J/\psi\eta_c(2S)$ and find no evidence for the process $e^+e^- \rightarrow J/\psi J/\psi$. We have calculated the cross sections for $e^+e^- \rightarrow J/\psi\eta_c$, $J/\psi\chi_{c0}$, and $J/\psi\eta_c(2S)$ with better statistical accuracy and reduced systematic errors and set an upper limit for $\sigma(e^+e^- \rightarrow J/\psi J/\psi) \times \mathcal{B}(J/\psi \rightarrow >2 \text{ charged})$ of 9.1 fb at the 90% CL. Although this limit is not inconsistent with the prediction for the $J/\psi J/\psi$ rate given in Ref. [3], the suggestion that a large fraction of the inferred $J/\psi\eta_c$ signal consists of $J/\psi J/\psi$ events is ruled out. We have measured the production and helicity angle distributions for $e^+e^- \rightarrow J/\psi\eta_c$, $J/\psi\chi_{c0}$, and $J/\psi\eta_c(2S)$; the distributions are consistent with expectations for these states, and disfavor a spin-0 glueball contribution to the η_c peak. We observe $\psi(2S)(c\bar{c})_{\text{res}}$ production for the first time, and find that the pro-

duction rates for these final states are of the same magnitude as the corresponding rates for $J/\psi(c\bar{c})_{\text{res}}$.

We thank the KEKB group for the excellent operation of the accelerator, the KEK Cryogenics group for the efficient operation of the solenoid, and the KEK computer group and the NII for valuable computing and SuperSINET network support. We acknowledge support from MEXT and JSPS (Japan); ARC and DEST (Australia); NSFC (Contract No. 10175071, China); DST (India); the BK21 program of MOEHRD and the CHEP SRC program of KOSEF (Korea); KBN (Contract No. 2P03B 01324, Poland); MIST (Russia); MESS (Slovenia); NSC and MOE (Taiwan); and DOE (USA).

-
- [1] Belle Collaboration, K. Abe *et al.*, Phys. Rev. Lett. **89**, 142001 (2002).
- [2] E. Braaten and J. Lee, Phys. Rev. D **67**, 054007 (2003); predictions for the angular distributions are listed in the appendix.
- [3] G. T. Bodwin, J. Lee, and E. Braaten, Phys. Rev. Lett. **90**, 162001 (2003).
- [4] S. J. Brodsky, A. S. Goldhaber, and J. Lee, Phys. Rev. Lett. **91**, 112001 (2003).
- [5] S. Dulat, K. Hagiwara, and Z. H. Lin, hep-ph/0402230.
- [6] Belle Collaboration, A. Abashian *et al.*, Nucl. Instrum. Methods Phys. Res., Sect. A **479**, 117 (2002).
- [7] S. Kurokawa and E. Kikutani, Nucl. Instrum. Methods Phys. Res., Sect. A **499**, 1 (2003).
- [8] The MC sample for the efficiency study is generated assuming a $(1 + \cos^2\theta_{\text{prod}}) \times (1 + \cos^2\theta_{\text{hel}})$ distribution for $J/\psi\eta_c$ and $J/\psi\eta_c(2S)$ final states, and a $(1 - \cos^2\theta_{\text{prod}}) \times (1 - \cos^2\theta_{\text{hel}})$ distribution for $J/\psi\chi_{c0}$. This choice is motivated by the subsequent angular distribution study.
- [9] E. Kuraev and V. Fadin, Sov. J. Nucl. Phys. **41**, 466 (1985).